Article

HET

Human and Experimental Toxicology
2016, Vol. 35(10) 1123–1132

DOI: 10.1177/0960327115622258
het.sagepub.com
SAGE

Toxicological evaluation of Prussian blue nanoparticles after short exposure of mice

Y Chen[1,2], L Wu[1,2], Q Wang[1,2], M Wu[1,2], B Xu[1,2], X Liu[1,2] and J Liu[1,2,3]

Abstract

Prussian blue nanoparticle (PBNP), a new type of theranostic nanomaterial, had been used for cancer magnetic resonance imaging and photothermal therapy. However, their long-term toxicity after short exposure in vivo was still unclear. In this study, we investigated the dynamic changes of the biochemical and immunity indicators of mice after PBNPs injection through tail vein. Histological results showed that the PBNPs were mainly accumulated in liver and spleen. In the spleen, we found the frequency of T cells was starting to decrease after 1 day of PBNPs injection, but then slowly recovered to normal level after 60 days of injection. Meanwhile, the frequency of T cells in the blood was firstly decreased after the PBNPs injection, and then the T cell frequency kept increasing and recovered back to normal levels after 7 days of injection. The serum indexes of liver functions (alanine transaminase, aspartate transaminase, total bilirubin, and alkaline phosphatase) increased rapidly to a relatively high level only after 1 h of injection, which meant certain acute liver damage, but these indexes were gradually decreased to normal levels after 60 days of injection. These results indicate that PBNPs have acute toxicity in vivo, however, their long-term toxicity after short-time exposure is low, which might provide guidance for further applications of PBNPs in future.

Keywords

Prussian blue nanoparticles, biodistribution, immunity, toxicity

Introduction

Prussian blue, a dye with long history, has been widely used in many fields such as optical physics, magnetism, and electrochemical for its excellent properties.[1–3] Prussian blue, certificated by Food and Drug Administration for treating thallium radiation poisoning, also has been used as a conventional drug in hospital.[4] In recent years, Prussian blue nanoparticles (PBNPs) have attracted much attention due to their excellent photothermal and imaging abilities and have been widely used in biomedical fields such as biosensor, cancer photothermal therapy, and magnetic resonance (MR) imaging.[5,6] For example, Liang et al. applied Prussian blue-coated gold and iron oxide nanoparticles for imaging-guided photothermal cancer ablation in mouse model;[7,8] Cheng et al. applied polyethylene glycol-modified PBNPs as a theranostic agent, which could be highly uptaken by tumor cells under various physiological conditions.[9] In our

[1]The United Innovation of Mengchao Hepatobiliary Technology Key Laboratory of Fujian Province, Mengchao Hepatobiliary Hospital of Fujian Medical University, Fuzhou, People's Republic of China
[2]The Liver Center of Fujian Province, Fujian Medical University, Fuzhou, People's Republic of China
[3]Liver Disease Center, The First Affiliated Hospital of Fujian Medical University, Fuzhou, People's Republic of China

Corresponding authors:
X Liu, The United Innovation of Mengchao Hepatobiliary Technology Key Laboratory of Fujian Province, Mengchao Hepatobiliary Hospital of Fujian Medical University, Fuzhou 350025, People's Republic of China.
Email: xiaoloong.liu@gmail.com
Jingfeng Liu, The United Innovation of Mengchao Hepatobiliary Technology Key Laboratory of Fujian Province, Mengchao Hepatobiliary Hospital of Fujian Medical University, Fuzhou 350025, People's Republic of China.
Email: drjingfeng@126.com

previous study, we functionalized PBNPs with Glypican-3 antibody for targeted MR imaging and photothermal therapy of hepatocellular carcinoma[10] and fabricated hollow PBNPs for combining chemotherapy and photothermal therapy.[11] However, long-term toxicity of PBNPs after short exposure in vivo is a key issue for biomedical applications. So far, the biodistribution, metabolism, and long-term toxicity of the PBNPs after short exposure in vivo is still unclear. Hence, we here systematically studied the long-term toxicity after short exposure and immunity responses of PBNPs in vivo, which might provide further valuable information for the biochemical applications of PBNPs.

Materials and methods

Animals

Female Balb/c mice of clean grade were purchased from the Experimental Animal Center of Fujian Medical University, China (License No: SCXKmin 2012-0002). Their average weight at the time of study was 22 ± 3 g. All mice were fed with a commercial diet and given water as needed. Room temperature was maintained at 18–20°C and relative humidity at 55 ± 10%. All animal procedures performed were approved by the Institutional Animal Care and Use Committee of Fujian Medical University, and thus within the guidelines for human care of laboratory animals for scientific purposes.

Preparation of PBNPs

PBNPs were prepared according to literature with modification.[12] Typically, 6 g polyvinylpyrrolidon (molecular weight: 58,000) and 0.1131 g potassium ferricyanide were added to hydrochloric acid solution (80 mL, 0.01 M) in a flask under magnetic stirring. After 1 h, the solution was heated at 80°C and refluxed for 20 h. The systems were then allowed to naturally cool to room temperature. The final precipitates were collected by centrifugation (50,000*g*, 20 min), washed with distilled water three times, and dried in vacuum at 50°C to obtain the PBNPs. The morphology and particle size of the prepared samples were characterized by scanning electron microscopy (SEM, Hitachi Limited, Japan) and transmission electron microscopy (TEM, Tecnai G20, FEI Co., Hillsboro, Oregon, USA), respectively. The average hydrodynamic size of PBNPs was determined by dynamic light scattering (DLS) experiments, which were performed at 25°C on a NanoZS (Malvern Instruments, Malvern, UK) with a detection angle of 173° and a 3 mW helium–neon laser operating at a wavelength of 633 nm. The Z-Average diameter and the polydispersity index values were obtained from analyzing the correlation functions through cumulative analysis.

Treatment regimen

Prussian nanoparticles were dissolved in phosphate-buffered saline (PBS) at the concentration of 400 μg/mL by sonication. Thirty female Balb/c mice were randomly divided into six groups and injected with 500 μL Prussian nanoparticles at the concentration of 8 mg/kg through the tail vein (five mice per group). Another five female Balb/c mice were injected with 500 μL PBS as control. At different time points (1 h, 6 h, 1 day, 3 days, 7 days, and 60 days), mice were killed and blood samples were collected by retro orbital puncture. Then the liver, the spleen, and other tissues, such as the kidney, the intestine, and so on, were all collected for histological and biochemical examinations.

Slicing and staining

Tissues were fixed by 10% formalin over 10 h. Afterward, they were paraffin-embedded, sliced, and stained by eosin since the color of PBNPs itself was blue.

Image acquisition

The images of interested organs were taken by Nikon digital camera. Bright-field images of eosin-stained tissue slices were visualized with a Leica DMI4000 B microscope (Germany) and the images were taken by the digital image acquisition system of the microscope at 40× magnification.

Flow cytometry analysis

Flow cytometry analysis was performed on FACS Canto II (BD Biosciences, San Diego, California, USA) with BD FACSuite (Version 1.0, USA) using directly conjugated monoclonal antibodies against the following markers: CD3-Alexa 647, CD45-PerCP, CD4-FITC, and CD8-PE (BD Biosciences).

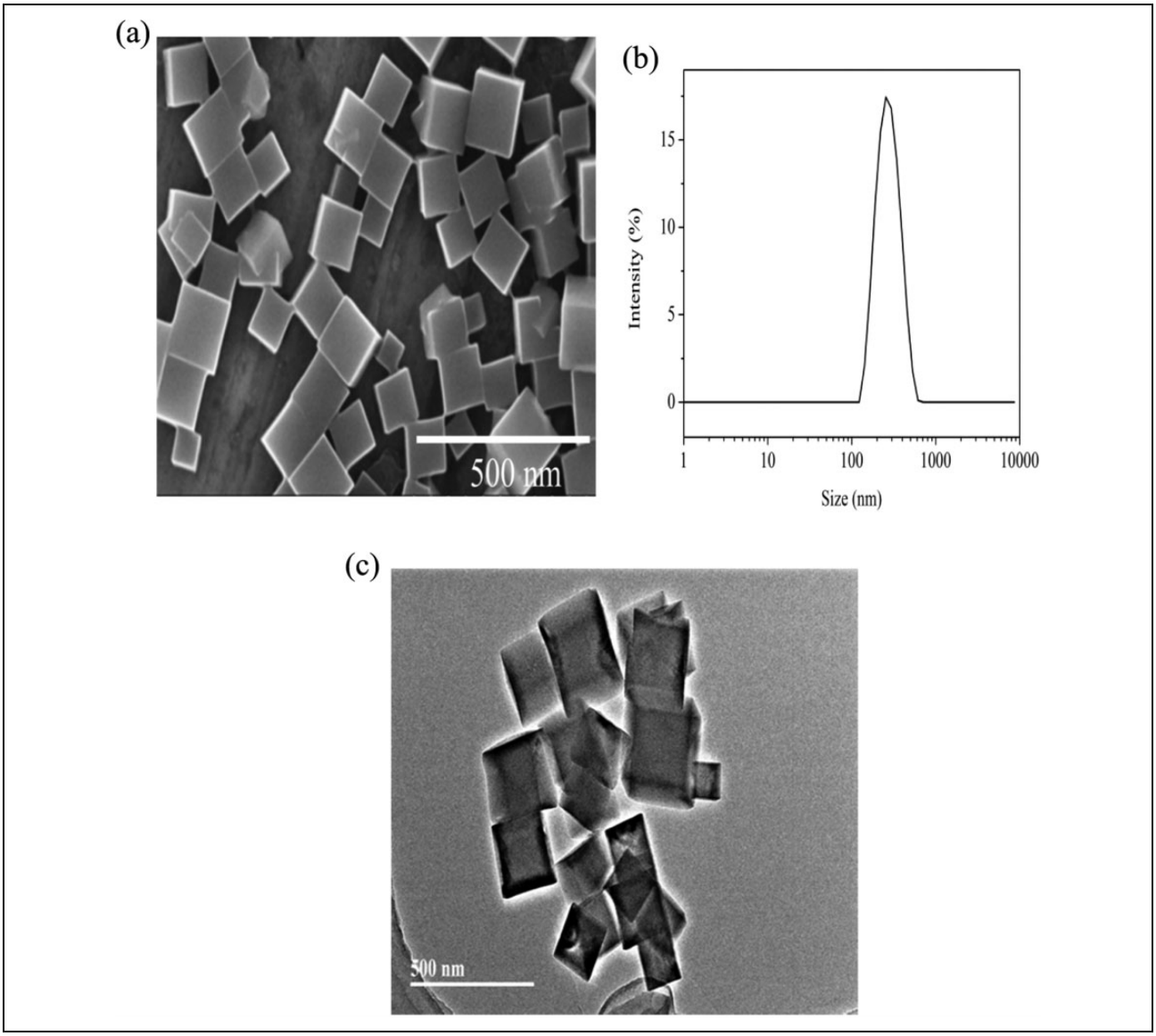

Figure 1. (a) SEM micrograph of PBNPs; the mean diameter was 100 nm (scale bar = 500 nm). (b) The average hydrodynamic size of PBNPs determined by the DLS experiments. (c) TEM micrograph of PBNPs (scale bar = 500 nm). SEM: scanning electron microscopy; PBNP: Prussian blue nanoparticle; DLS: dynamic light scattering; TEM: transmission electron microscopy.

Measurement of biochemical indexes

Blood was collected from the orbital sinus. After centrifugation at 2000*g* for 10 min, the supernatant was collected and measured by a autobiochemical analyzer (Abbott company; Chicago, Illinois, USA). The reagents were from Abbott laboratories (3L82-21).

Statistical analysis

The statistical analysis was carried out with GraphPad (GraphPad Software Inc., San Diego, California, USA). Data from at least five experiments were expressed as mean value $\pm$ standard deviation and interpreted by analysis of variance test. All variables were determined by a repeated measure analysis of variance between the injected group and the control group.

Results

SEM images indicated that the average particle size of the original PBNPs was around 100 nm and the uniform cubic structure is shown in Figure 1(a). The average hydrodynamic size of the PBNPs was 251.7 nm as determined by the DLS experiments (Figure 1(b)).

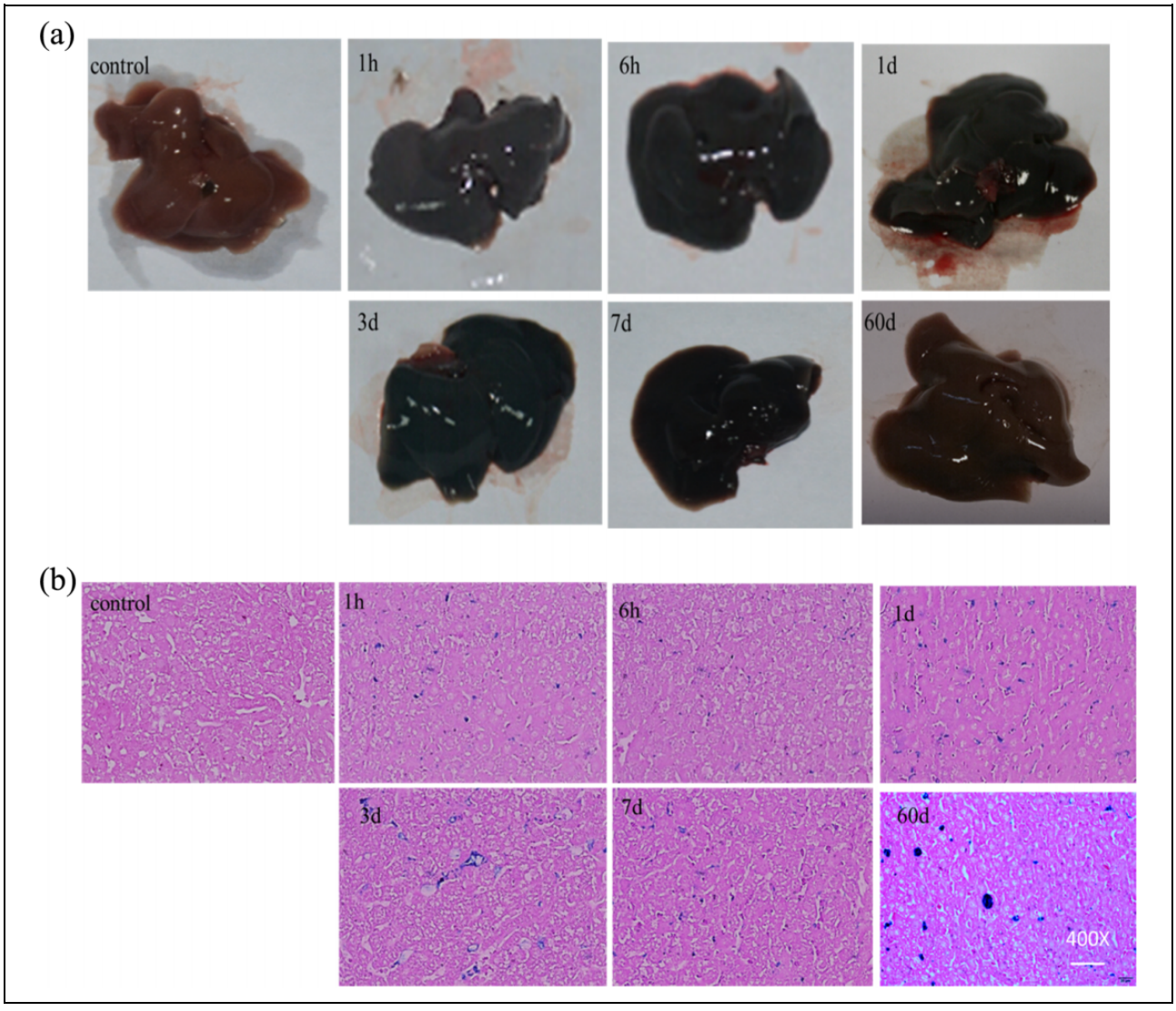

Figure 2. Histological changes of the liver at different time point after PBNPs injection (8 mg/kg Prussian nanoparticles). (a) The photos of the collected liver at the indicated time point. (b) The images of eosin-stained liver sections at the indicated time point. Control, which means the liver from none-injected mice. PBNPs: Prussian blue nanoparticles.

The cubic structure of PBNPs could also be observed in TEM image and their diameter was consistent with those determined by SEM (Figure 1(c)).

Survival and mouse living status

In this model, the animals would survive for more than 60 days after injection of PBNPs at the dose of 8 mg/kg. After injection of PBNPs for about 1 h, some minor side effects including drowsiness and loss of appetite happened. These symptoms gradually disappeared and the status of the animals recovered to normal till the third day after injection.

Histological changes

First the biodistribution of PBNPs was carefully examined in vivo. Female Balb/c mice were killed at 1 h, 6 h, 1 day, 3 days, 7 days, and 60 days post-injection of PBNPs (8 mg/kg) and various organs and tissues were collected, sliced, and stained by eosin at the mean time (Figures 2 and 3). It was found that PBNPs were distributed in many different organs and mainly accumulated in the liver and spleen at above-indicated time point after injection. From Figures 2 and 3, we could clearly see that the color of the liver and spleen turned more and more blue and the numbers of blue spots were increased in the tissue section till 3 days, suggesting the gradual

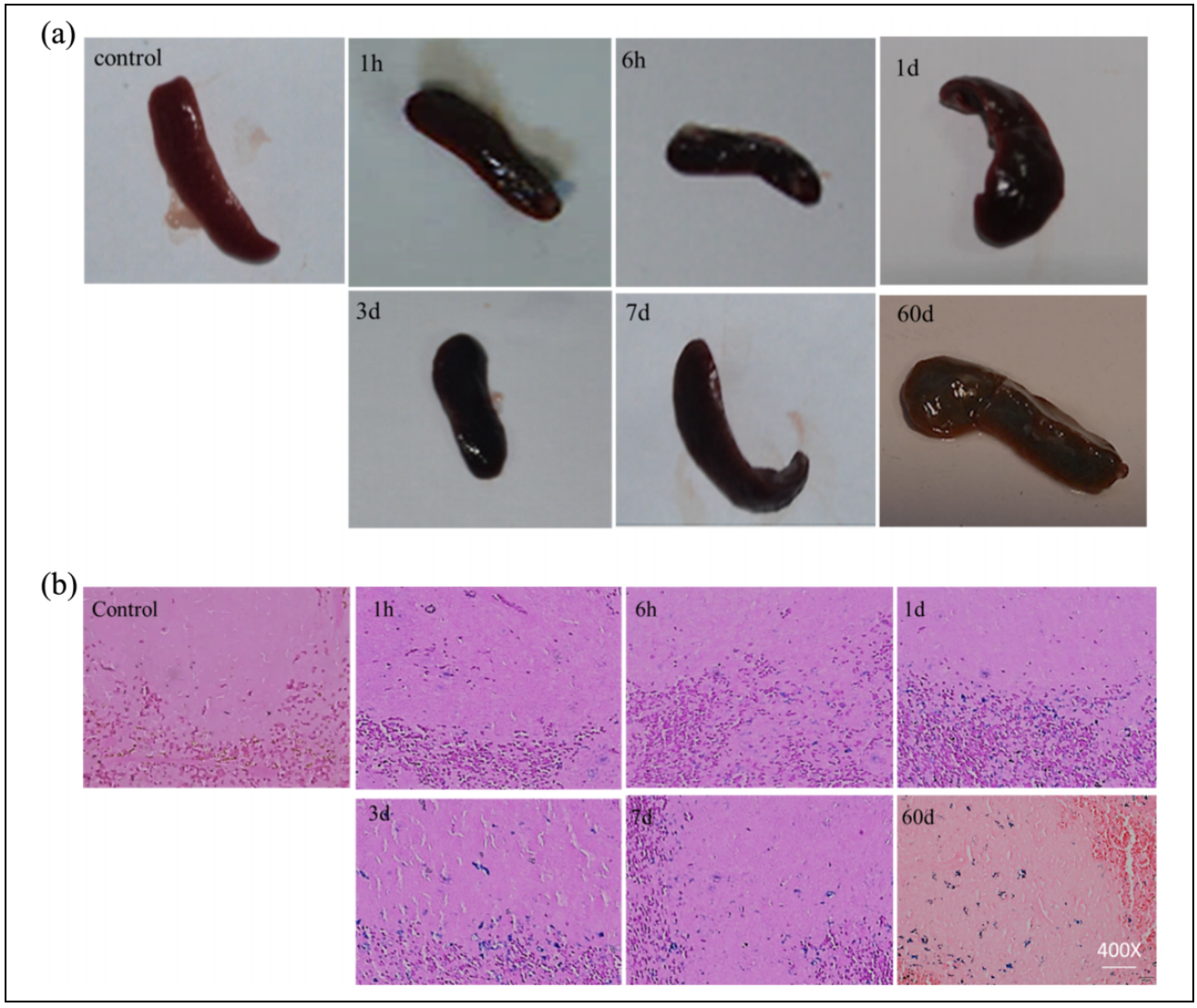

Figure 3. Histological changes of the spleen at different time points after PBNPs injection (8 mg/kg Prussian nanoparticles). (a) The photos of the collected spleen at the indicated time point. (b) The images of eosin-stained spleen sections at the indicated time point. Control, which means the liver from none-injected mice. PBNPs: Prussian blue nanoparticles.

accumulation of PBNPs. However, the accumulated PBNPs could be gradually metabolized or excreted by the liver and spleen, since the color of both organs and the numbers of blue spots in the sliced sections were gradually decreased from the third day post-injection. The color of the organs was recovered to normal after 7 days of injection, but we could still see several blue spots and dispersed particles in the section of liver and spleen even after 60 days of injection. These results showed that the PBNPs could be metabolized, though it is very difficult to be completely removed from the body.

Analysis of $CD3^+CD4^+$ T cells and $CD3^+CD8^+$ T cells in the liver

$CD3^+$ T cells, $CD3^+CD4^+$ T cells, and $CD3^+CD8^+$ T cells are the key cell populations of immune responses.[13] To investigate the immune response in the liver after the injection of PBNPs, these cell numbers and frequencies were carefully analyzed. In the liver, the T cell numbers ($CD3^+$) and frequencies of $CD3^+CD4^+$ T cells and $CD3^+CD8^+$ T cells were very limited (Figure 4). Meanwhile, there were no significant differences among different time points (1 h, 6 h, 1 day, 3 days, 7 days, and 60 days) after injection of PBNPs.

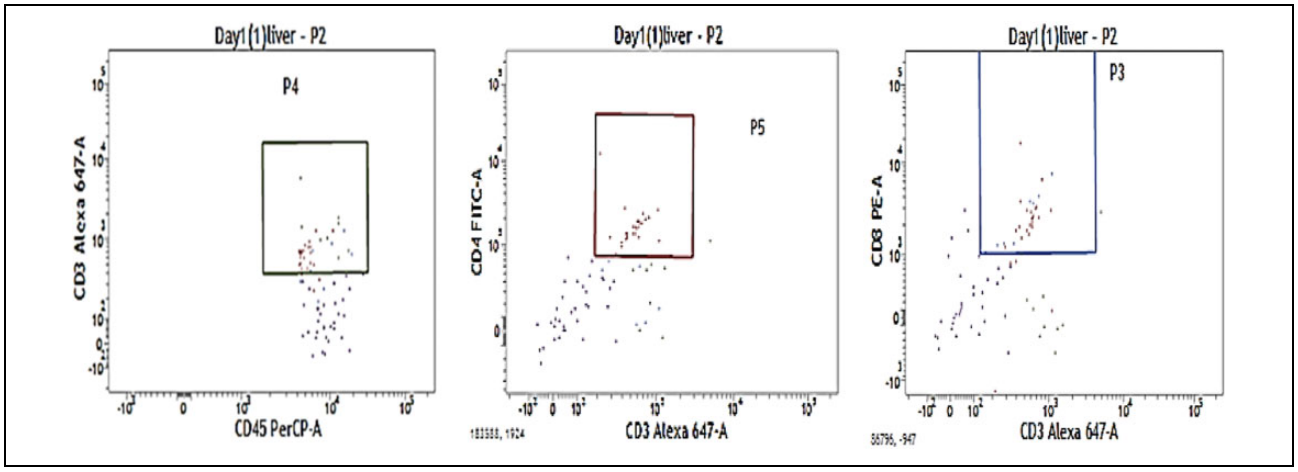

Figure 4. The FACS analysis of $CD3^+$ T cells, $CD3^+CD4^+$ T cells, and $CD3^+CD8^+$T cells in the liver. FACS: fluorescence-activated cell sorting.

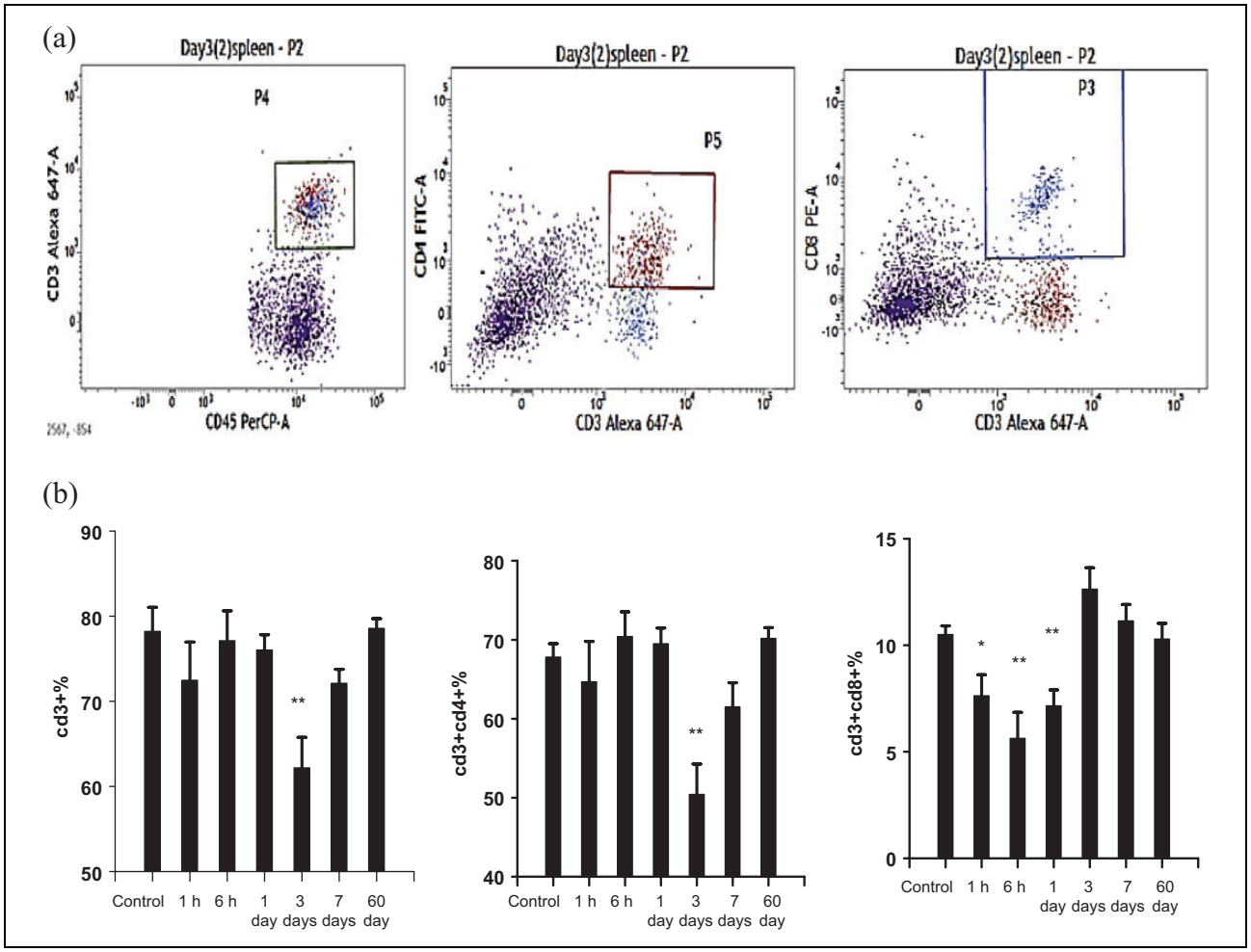

Figure 5. The FACS analysis of $CD3^+$ T cells, $CD3^+CD4^+$ T cells, and $CD3^+CD8^+$T cells in the spleen. (a) The spot plot of the indicated cells. (b) The statistical analysis of the cell populations. $^*p < 0.05$; $^{**}p < 0.01$. FACS: fluorescence-activated cell sorting.

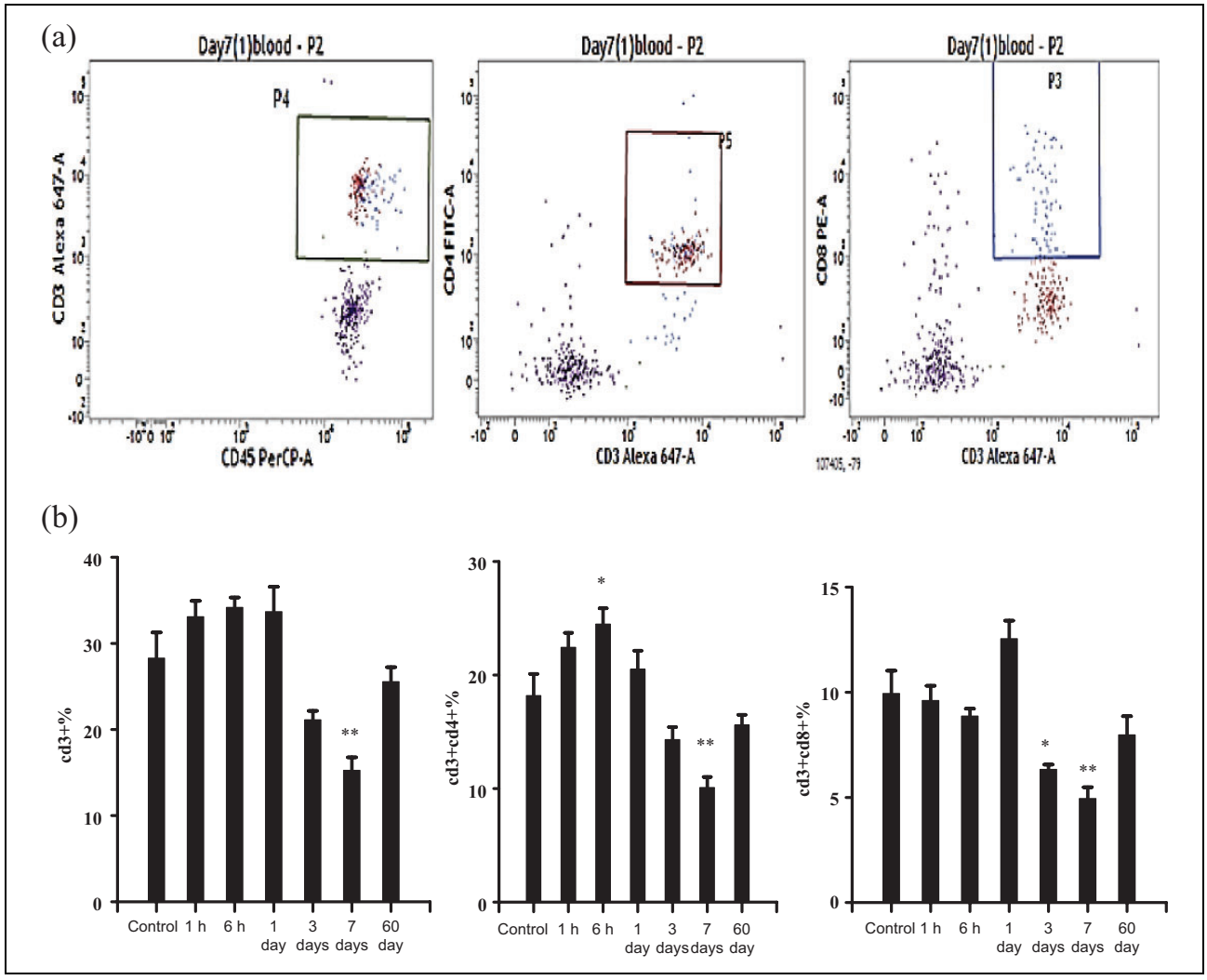

Figure 6. The FACS analysis of $CD3^+$ T cells, $CD3^+CD4^+$ T cells, and $CD3^+CD8^+$T cells in the blood. (a) The spot plot of the indicated cells. (b) The statistical analysis of the cell populations. *$p < 0.05$; **$p < 0.01$. FACS: fluorescence-activated cell sorting.

Analysis of $CD3^+CD4^+$ T cells and $CD3^+CD8^+$ T cells in the spleen

To investigate the immune response in the spleen after PBNP injection, the cell numbers and frequencies of $CD3^+$ T cells, $CD3^+CD4^+$ T cells, and $CD3^+CD8^+$ T cells in the spleen were carefully analyzed (Figure 5). The percentage of $CD3^+$ T cells and $CD3^+CD4^+$ T cells in the spleen rapidly increased right after 1 h of PBNPs injection and they reached the peak after 1 day of injection. However, the $CD3^+CD8^+$ T cells were slightly decreased right after 1 h of PBNP injection, increased after 6 h of injection, and reached the peak after 1 day of injection. Afterwards, all cell populations ($CD3^+$ T cells, $CD3^+CD4^+$ T cells, and $CD3^+CD8^+$ T cells) started decreasing till the 1st day. But after 60 days of injection, the percentage of all cell populations was recovered back to nearly normal level. These results indicated that T cell immune responses were triggered in short time, but these effects did not sustain a long time.

Analysis of $CD3^+CD4^+$ T cells and $CD3^+CD8^+$ T cells in the blood

To investigate the immune response in the blood after PBNP injection, the cell numbers and frequencies of $CD3^+$ T cells, CD3+CD4+T cells, and CD3+CD8+T cells in the blood were carefully analyzed (Figure 6). On the first day post-injection, the percentage of $CD3^+$ T cells and $CD3^+CD4^+$ T cells

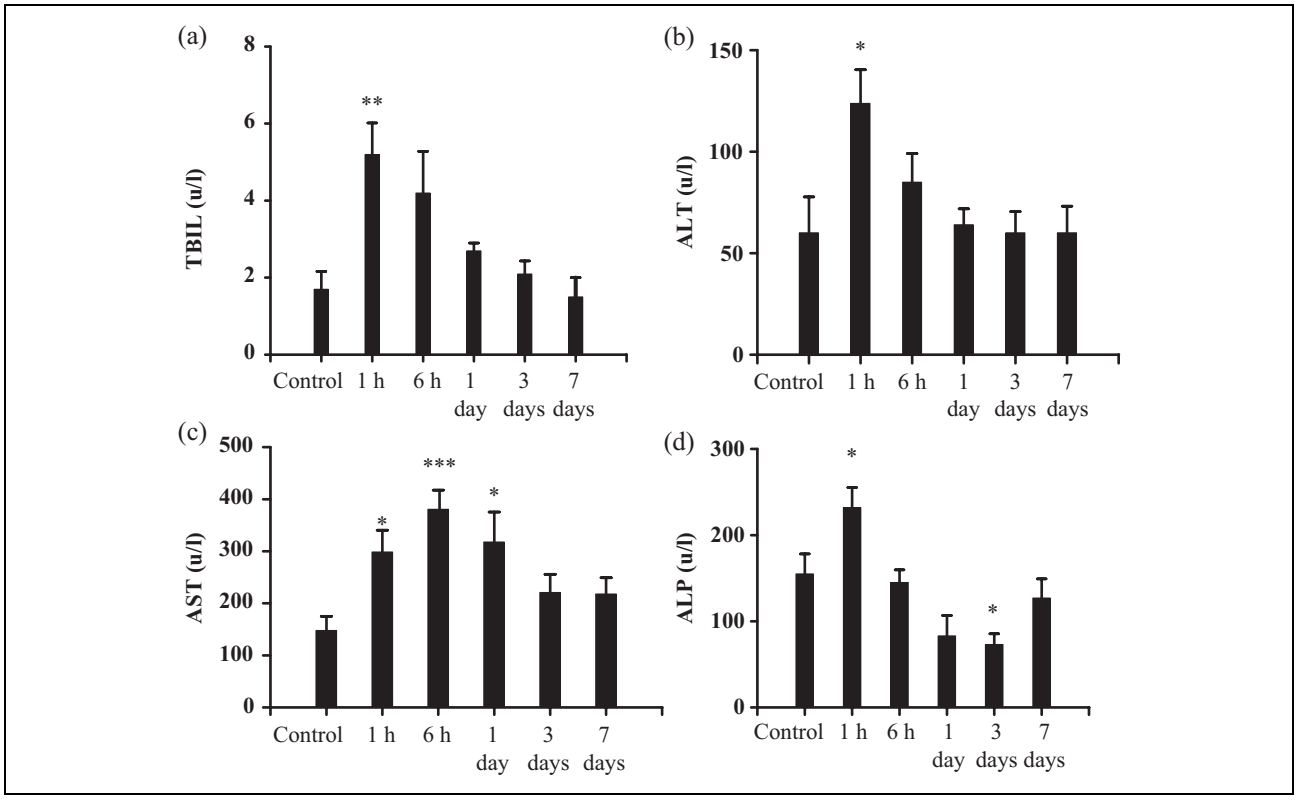

Figure 7. Analysis of the biochemical indicators in the blood. (a) Tbil, (b) ALT, (c) AST, and (d) ALP. *$p < 0.05$. **$p < 0.01$. ***$p < 0.001$. FACS: fluorescence-activated cell sorting. Tbil: total bilirubin; ALT: alanine transaminase; AST: aspartate transaminase; ALP: alkaline phosphatase.

were not obviously decreased in the blood. After 3 days of injection, the $CD3^+$ T cells and $CD3^+CD4^+$ T cells were significantly decreased to almost 50%; however, the cell numbers and percentages were starting to recover after the 3rd day and almost recovered to normal level after 60 days. The $CD3^+CD8^+$ T cells were starting to decrease right after 1 h of PBNP injection and reached its bottom after 6 h of injection, and then the $CD3^+CD8^+$ T cell numbers and percentages were starting to recover and reached back to normal level after 7 days of injection. These results indicated that T cell immune functions in the blood were completely recovered within the analyzed time frame.

Analysis of biochemical indexes in the blood

To investigate the toxic effects of PBNPs in the injected mice, blood biochemistry and hematology analysis were carried out. The serum indexes of liver functions including total bilirubin (Tbil), alanine transaminase (ALT), aspartate transaminase (AST), and alkaline phosphatase (ALP) were dramatically increased after 1 h of PBNP injection. Afterwards, all of these indexes were slowly decreased to normal level (Figure 7).

Discussion

PBNPs have been widely used in biomedical field, such as biosensor, MR imaging, and cancer photothermal therapy in vitro and in vivo.[14–16] In the practice, the biosafety of PBNPs is very important for its biomedical applications.

Our results pointed out that the PBNPs have little impact on mice survival, and the PBNPs were mainly accumulated in the reticuloendothelial system such as liver and spleen after injection through tail vein. The biological effects of PBNPs at different time points concluded that PBNPs had acute toxicity but the long-term toxicity after short exposure is low. Compared with biochemical response, immune response could also be used to evaluate the toxic effect of PBNPs.[17] Our data showed that T cells were very limited in the liver and the impact on liver immune function was hard to be evaluated.[18] In the spleen, the results suggested that the T cells that were born in the spleen could be damaged by the accumulated PBNPs.

The data of impact on T cell immunity in the spleen and in the blood indicated that PBNPs had acute toxicity to spleen while the long-term toxicity after short exposure is low. Finally, the serum indexes of liver functions, such as Tbil, ALT, AST, and ALP suggest that at the beginning PBNPs have acute toxicity to the body while no long-term toxicity is observed, indicating that the PBNPs are relatively safe.

Previous study of the toxicities in vivo were mainly through the histological staining of sections and measuring of biochemical indexes.[19,20] For example, Liang et al. evaluated the histological changes of the heart, liver, spleen, lung, and kidneys by hematoxylin and eosin (HE) staining and found no apparent injury to cellular structure after the injection of PBNPs.[21] While the PBNPs were blue themselves, it would overlap with the color of HE staining because the cell nucleus was also stained with blue by hematoxylin. Therefore, the histological sections were only stained by eosin in our experiment to avoid color interference with each other. Meanwhile, we also carefully analyzed the impact of PBNPs on the immune system at different time points in 60 days rather than only examination of the histological changes and biochemical changes.

In conclusion, we carefully investigated the biodistribution of PBNPs in vivo and analyzed the impact of PBNPs on the immune system and on the liver functions in vivo. The results show that the PBNPs have acute toxicity to both the immune system and the liver, but the damage could be gradually recovered due to the metabolism and excretion of the nanoparticles. Therefore, the PBNPs have very low long-term toxicity after short exposure to the body and might be a relatively safe nanomaterial for biomedical applications. The study here could provide further information and guidance for the development of better Prussian blue-based nanomaterials in the future.

Declaration of Conflicting Interests

The author(s) declared no potential conflicts of interest with respect to the research, authorship, and/or publication of this article.

Funding

The author(s) disclosed receipt of the following financial support for the research, authorship, and/or publication of this article: This work is supported by the scientific innovation project of Fujian provincial Health and Family Planning Commission (Grant No. 2014-CX-32).

References

1. Omura A, Tanaka H, Kurihara M, et al. Electrochemical control of the elution property of Prussian blue nanoparticle thin films: mechanism and applications. *Phys Chem Chem Phys* 2009; 11(44): 10500–10505.
2. Lee DY, Kafi AK, Choi WS, et al. Glucose sensor based on glucose oxidase-lipid LB film immobilized in Prussian blue layer. *J Nanosci Nanotechnol* 2008; 8(9): 4543–4547.
3. Suwansa-Ard S, Xiang Y, Bash R, et al. Prussian blue dispersed sphere catalytic labels for amplified electronic detection of DNA. *Electroanalysis* 2008; 20(3): 308–312.
4. Miller MA, Patel MM, and Coon T. Prussian blue for treatment of thallium overdose in the US. *Hospital Pharmacy* 2005; 40: 796–797.
5. Zhang W, Ma D, and Du J. Prussian blue nanoparticles as peroxidase mimetics for sensitive colorimetric detection of hydrogen peroxide and glucose. *Talant* 2014; 120: 362–367.
6. Gao L, He J, Xu W, et al. Ultrasensitive electrochemical biosensor based on graphite oxide, Prussian blue, and PTC-NH2 for the detection of α2,6-sialylated glycans in human serum. *Biosens Bioelectron* 2014; 62: 79–83.
7. Jing L, Liang X, Deng Z, et al. Prussian blue coated gold nanoparticles for simultaneous photo acoustic/CT bimodal imaging and photothermal ablation of cancer. *Biomaterials* 2014; 35: 5814–5821.
8. Fu G, Liu W, Li Y, et al. Magnetic Prussian blue nanoparticles for targeted photothermal therapy under magnetic resonance imaging guidance. *Bioconjug Chem* 2014; 25: 1655–1663.
9. Cheng L, Gao H, Zhu WW, et al. PEGylated Prussian blue nanocubes as a theranostic agent for simultaneous cancer imaging and photothermal therapy. *Biomaterial* 2014; 35: 9844–9852.
10. Li ZL, Zeng YY, Zhang D, et al. Glypican-3 antibody functionalized Prussian blue nanoparticles for targeted MR imaging and photothermal therapy of hepatocellular carcinoma. *J Mater Chem B* 2014; 2: 3686–3696.
11. Wu M, Wang QT, Liu XL, et al. Highly efficient loading of doxorubicin in Prussian blue nanocages for combined photothermal/chemotherapy against hepatocellular carcinoma. *RSC Adv* 2015; 5: 30970–30980.
12. Hu M, Furukawa S, Ohtani R, et al. Synthesis of Prussian blue nanoparticles with a hollow interior by controlled chemical etching. *Angew Commun* 2012; 51: 984–988.
13. Trautmann T, Kozik JH, Carambia A, et al. CD4+ T-cell help is required for effective CD8+ T

cell-mediated resolution of acute viral hepatitis in mice. *PLoSone* 2014; 9: e86348.
14. Hoffman HA, Chakrabarti L, Dumont MF, et al. Prussian blue nanoparticles for laser-induced photothermal therapy of tumors. *RSC Adv* 2014; 4: 29729–29734.
15. Banerjee S, Sarkar P, and Turner AP. Amperometric biosensor based on Prussian blue nanoparticle-modified screen-printed electrode for estimation of glucose-6-phosphate. *Anal Biochem* 2013; 439: 194–200.
16. Fu G, Liu W, Feng S, et al. Prussian blue nanoparticles operate as a new generation of photothermal ablation agents for cancer therapy. *Chem Commun* 2012; 48: 11567–11569.
17. Germain RN. T-cell development and the CD4–CD8 lineage decision. *Nat Rev Immunol* 2002; 2: 309–322.
18. Huang X, Zou Y, Lian L, et al. Changes of T cells and cytokines TGF-β and IL-10 in mice during liver metastasis of colon carcinoma: implications for liver anti-tumor immunity. *J Gastronintest Surg* 2013; 17: 1283–1291.
19. Lam CW, James JT, and McCluskey R. Pulmonary toxicity of single-wall carbon nanotubes in mice 7 and 90 days after intratracheal instillation. *Toxocol Sci* 2004; 77: 126–134.
20. Cheng L, Yang K, Shao M, et al. In vivo pharmacokinetics, long-term biodistribution and toxicology study of functionalized upconversion nanoparticles in mice. *Nanomedicine* 2011; 6: 1327–1340.
21. Liang XL, Deng ZJ, Jing LJ, et al. Prussian blue nanoparticles operate as a contrast agent for enhanced photoacoustic imaging. *Chem Commun* 2013; 49: 11029–11031.